Low-Power Reflective Optical Communication System for Pico- and Nano-Satellites

Andreas Sinn, Thomas Riel, Florian Deisl, Rudolf Saathof and Georg Schitter

Automation and Control Institute, Vienna University of Technology
Gusshausstrasse 27-29, 1040 Vienna, Austria

ABSTRACT

Pico- and nano-satellites (PNS) are promising options for cost-effective and rapid deployable satellite systems. Due to their small size, the available power and therefore the transmittable data volume is limited. This paper proposes optical communication by means of reflected laser light using a modulating retro-reflector (MRR) for energy efficient optical communication with PNS. No laser source or beam steering assembly is necessary at the satellite, thus allowing a weight and energy efficient communication interface. Existing ground stations (GS) as used for satellite laser ranging (SLR) provide all equipment required for this system. By providing a link budget for communication to PNS in LEOs feasibility is investigated. It is shown that an affordable GS based on small telescopes with diameters below 0.3m in combination with commercial mounts enables the targeted application. A detailed analysis of LCD based MRRs is shown, denoting cost-efficient modulators for reflective optical communication. A data-rate of 2.5kbps at an input power of less than 80 mW is shown in a laboratory setup. Using a high performance sampling circuit and a laser power of only 1mW, a bit error ratio (BER) of below 10e-3 is achieved, successfully demonstrating reflective optical communication as an alternative to current RF based systems.

1. INTRODUCTION

Pico- and nano-satellites (PNS) offer a wide field of applications in space. Measurements of the lower thermosphere [1], earth observation [2] and technology demonstration [3] are only a few examples for the potential of PNS. Till 2020 more than 400 PNS launches per year are estimated [3]. These applications produce large amounts of data which need to be transmitted to the ground station (GS). Implementing a reliable, high data-rate communication link, while facing substantial limitations concerning power consumption is one of the major challenges of PNS.

One of the most energy consuming components of PNS is the communication subsystem [2]. Therefore, the transmittable amount of data is restricted to several Mega-bytes per day [4, 5]. Nevertheless, the amount of generated data on satellites is increasing with increased integration density and availability of detectors and data-processors. Consequently, these restrictions lead to the necessity of a faster and more energy-efficient communication system for PNS.
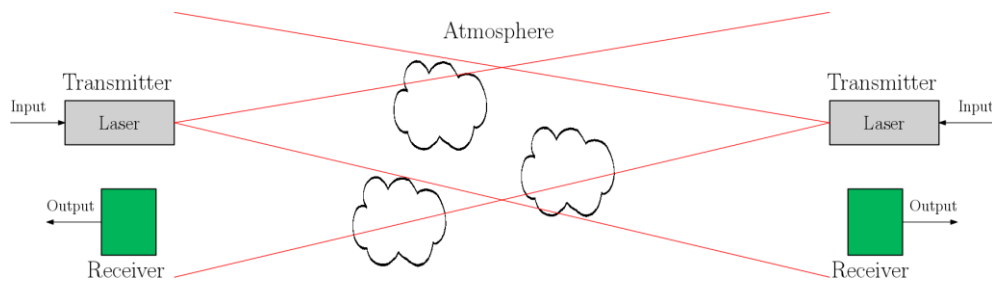

Fig. 1. Free space optical communication principle. The concept of FSO-C is to track the second communication participant with a modulated laser beam. This participant receives the transmitted information by means of a photo-detector. For bidirectional communication a laser source, as well as a pointing and tracking unit is required at both participants.

Conventional radio frequency (RF) communication is currently the most widely applied technique for the communication between satellites and ground stations (GS) [6]. However, due to legal restrictions and numerous communication participants, the available bandwidth is limited and costly [7]. To overcome these disadvantages free-space optical communication (FSO-C) has been proposed [5]. Fig. 1 shows the operating principle of FSO-C. Optical frequencies are freely usable and the variety of available components is high. They enable high speed communication

and allow very low divergence angles. Using these well focused beams, more energy can be concentrated at a smaller target area, thus increasing the efficiency and the SNR. Projects such as ARTEMIS [8] and Kirari [9] show the feasibility of this concept for bidirectional inter-orbit as well as bidirectional earth-orbit communication. However, these projects use satellites with masses of more than 500 kg and their communication modules exceed the weight, volume and power budgets of PNS [10]. In order to reduce the power and weight consumption of the communication module and to allow its integration into PNS, reflective free-space optical communication (R-FSO-C) has been proposed [5].
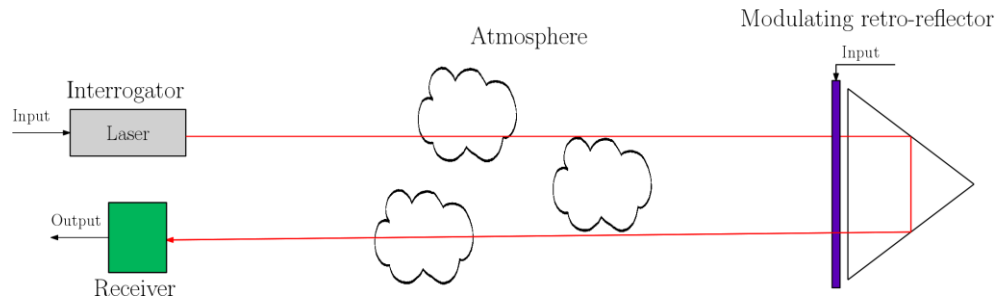

Fig. 2. Reflective free-space optical communication principle. The laser source and pointing and tracking unit at the satellite is replaced with a modulating retro-reflector (MRR). The MRR transmits information by modulating the retro-reflected laser beam. Tracking and illumination is provided by the GS. The usage of this MRR simplifies the pointing process and avoids an energy-intensive laser source at the satellite. All complex, large and power-consuming components are located at the ground station.

R-FSO-C allows the reduction of power consumption and weight at one of the participants (the satellite) by replacing the pointing and tracking unit and the laser source with a modulating retro-reflector (MRR). This assembly of a retro-reflector and a modulator reflects the incident laser beam directly back to its original source. The reflected beam is modulated and information is transmitted.

First experiments implementing R-FSO-C with UAVs have been done in 1992 [11]. Since then significant improvements in terms of link distance and data-rate have been achieved [12, 13, 14]. Several link-budgets promise the feasibility of reflective optical communication for low earth orbit (LEO) communication links [11, 13, 15]. However, the applicability of R-FSO-C for PNS has not yet been demonstrated. Due to the small size of the satellite additional limitations in terms of available space, weight and power challenge the R-FSO-C system. A more detailed analysis in terms of applicable modulating retro-reflector aperture size, power consumption, data-rates, tracking requirements and modulation concepts is required. This paper investigates the feasibility of R-FSO-C for PNS in low earth orbits. Two configurations are analyzed in simulation: A R-FSO-C system using a LCD based MRR with a maximum bitrate of 2.5 kbps and a multi-quantum well (MQW) based MRR system [16] with an exemplary bitrate of 1 Mbps. For the LCD-based MRR the simulation results are validated experimentally with indoor and outdoor measurements.

2. SYSTEM ANALYSIS AND REQUIREMENTS

The system analysis is used to identify crucial components and their properties. The aperture of the MRR, the necessary laser power and the telescope diameters are evaluated over the link distance. Fig. 3 shows a bistatic configuration, where transmitting and receiving is performed by two independent telescopes for analyzing the proposed R-FSO-C system and quantifying the link properties by simulation. The atmosphere is approximated by the LOWTRAN model [11]. Further parameters are the link distance L and the MRR's modulation bitrate BR. Θ_{RR} specifies the divergence angle introduced by the MRR. The receiver is characterized by its noise equivalent power (NEP) and the responsivity R. The optical notch filter is used to block straylight from different sources.
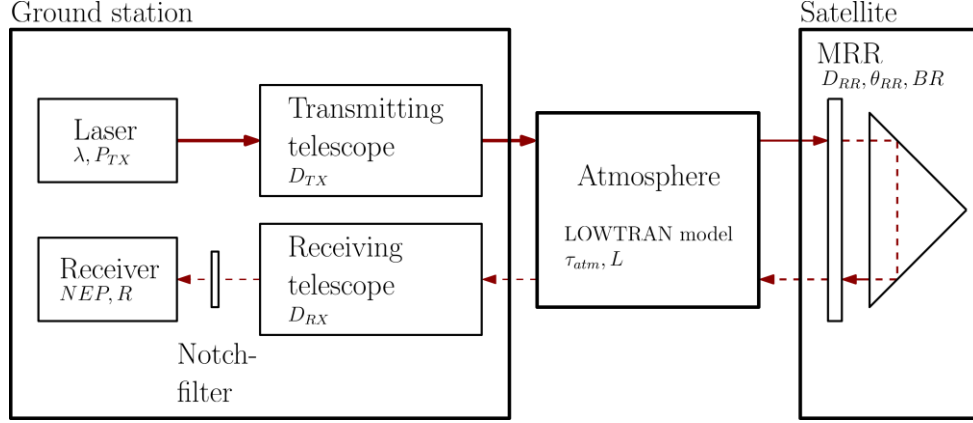
Fig. 3. Schematic setup of the R-FSO-C system used for the system analysis. Symbols and parameters according to Tab. 1. The pointing and tracking unit is not modeled in this simulation.

Tab. 1 lists the parameters which are used for the analysis. The aperture sizes of transmitter and receiver telescopes are in the range of standard, semi-professional telescope diameters. A Thorlabs APD120A2 is assumed as reference detector. The wavelength is chosen to be 840 nm, which is within one of the atmospheric transmission windows [17].

The system analysis is performed by calculating a link budget according to [11]. The atmospheric influences to the laser beam are modeled with the LOWTRAN atmospheric simulation model. It considers atmospheric absorption and scatter and allows to calculate properties such as the beam attenuation. Assuming a mid-latitude summer with light cirrus clouds and the given wavelength of 840 nm the model predicts a one-way attenuation of 35% [11].

$$\tau_{atm} = 0.65 \qquad (1)$$

Tab. 1. Hardware properties for the system analysis.

Parameter	Symbol	Value	Unit
Wavelength	λ	840	nm
Laser power	P_{TX}	5	W
Transmitter aperture	D_{TX}	0.3	m
MRR diameter	D_{RR}	2.54	cm
MRR divergence	Θ_{RRm}	20	µrad
Receiver aperture	D_{RX}	0.3	m
Link distance	L	300	km
Bitrate LCD	BR_{LCD}	2500	kbps
Bitrate MQW	BR_{MQW}	1	Mbps
Noise equivalent power	NEP	0.21	$pW/\sqrt{Hz}$
Receiver responsivity	R	25	A/W

Diffraction is the largest contributor to beam spreading. Three sources are considered: Transmitter aperture diffraction, MRR aperture diffraction and turbulence induced beam spread. Influences due to pointing and tracking of the satellite are not considered in this simulation, assuming that that for this first analysis these influences can be neglected. Aperture diffraction is modeled as Fraunhofer diffraction, which is given by

$$\theta = \frac{2.44\,\lambda}{D}, \qquad (2)$$

where θ is the divergence angle of the aperture specified with the diameter D. Beam spread due to atmospheric turbulences at ideal seeing conditions can be approximated to 2.4 µrad [11]. In order to take additional atmospheric disturbances during non-ideal seeing conditions into account this value is doubled to

$$\theta_{atm} = 4.8\,\mu rad. \qquad (3)$$

The attenuation of the upward beam due to beam spread is defined as

$$\tau_{up} = \frac{D_{RR}^2}{((\theta_{TX} + \theta_{atm}) \cdot L)^2}\;. \qquad (4)$$

The attenuation of the downlink beam is a combination of the upward beam spread, the retro-reflectors contribution and the atmospheric beam spread.

$$\tau_{down} = \frac{D_{RX}^2}{\left((\theta_{TX} + 2\theta_{atm} + \theta_{RR} + \theta_{RRm}) \cdot L\right)^2} \quad (5)$$

The optical components proposed, suffer from non-ideal properties. Tab. 2 specifies the transmittances and reflectivities assumed. Commercially available components are taken as reference. The overall beam attenuation due to optical losses is the product of every single attenuation and calculates as follows for the LCD (analog for the MQW)

Tab. 2. Optical properties of the components of the R-FSO-C system.

Parameter	Symbol	Value
TX optics transmittance	T_{TX}	0.9
Retro-reflector reflectivity	R_{RR}	0.9
LCD transmittance (opaque)	T_{LCD_OP}	0.02
LCD transmittance (clear)	T_{LCD_CL}	0.6
MQW transmittance (opaque)	T_{MQW_OP}	0.2
MQW transmittance (clear)	T_{MQW_CL}	0.8
RX optic transmittance	T_{RX}	0.9
Notch filter transmittance	T_{NOTCH}	0.6

$$\tau_{optical} = T_{TX} \cdot T_{LCD} \cdot R_{RR} \cdot T_{LCD} \cdot T_{RX} \cdot T_{NOTCH}. \quad (6)$$

The total attenuation is the product of all attenuation factors introduced above

$$\tau_{total} = \tau_{optical} \cdot \tau_{up} \cdot \tau_{atm} \cdot \tau_{down} \cdot \tau_{atm}, \quad (7)$$

leading to a power P_{RX} at the receiver of

$$P_{RX} = \tau_{total} \cdot P_{TX}. \quad (8)$$

Using the NEP of the receiver and the bandwidth BR, the receiver noise power P_N is calculated to

$$P_N = NEP \cdot \sqrt{BR}, \quad (9)$$

leading to the SNR which is the ratio between received power and total noise power (sum of receiver and background noise)

$$SNR = \frac{P_{RX}}{P_N + P_{BG}}. \quad (10)$$

The background radiation power P_{BG} collected by the receiving telescope is calculated for a field of view of the telescope of 560 arcsec and a background radiation magnitude of 18 [18, 19]. A notch filter with 20 nm FWHM at the used wavelength is assumed. It can be seen, that the intended link distance of 300 km is challenging but feasible with higher laser powers (> 5W).

In Fig. 4. the SNR is plotted as a function of the link distance. Due to the reduced data-rate of the LCD as compared to the MQW the SNR of the LCD is higher, since more photons per bit are received. For the smaller telescope diameter of 0.3 m the simulation indicates a SNR for the MQW-MRR of 14 dB at a link distance of 300 km. The SNR of the LCD-MRR is 24 dB at 300 km distance. Using on/off-keying modulation in non-return to zero mode these SNRs allow BERs of 31e-3 (MQW) and 7e-3 (LCD) [20]. Considering the facts, that off-the-shelf components and non-ideal atmospheric conditions are assumed for this simulation, these BER values are put into perspective. The feasibility of the R-FSO-C system for PNS seems plausible with LCD-MRR as well as MQW-MRR. Using the MQW-MRR the typical data-rate available for PNS can be increased by a factor of up to 20 to a value of 1 Mbps [21].

The received power at the detector increases with the fourth power of the retro-reflector's diameter [5]. Therefore, one of the most important trade-offs is the relation between MRR aperture size and maximum modulation speed of the modulator. For many modulator types (e.g. MQW) the maximum modulation speed is indirectly proportional to their active area [22]. Segmentation of the modulator area into several sub-pixels with independent drivers but the same signal pattern, reduces this restriction and allows higher bandwidth at large MRR aperture sizes [23]. Robustness and data-rate can be improved further by increasing the transmitted laser power and using larger transmitting and receiving aperture.
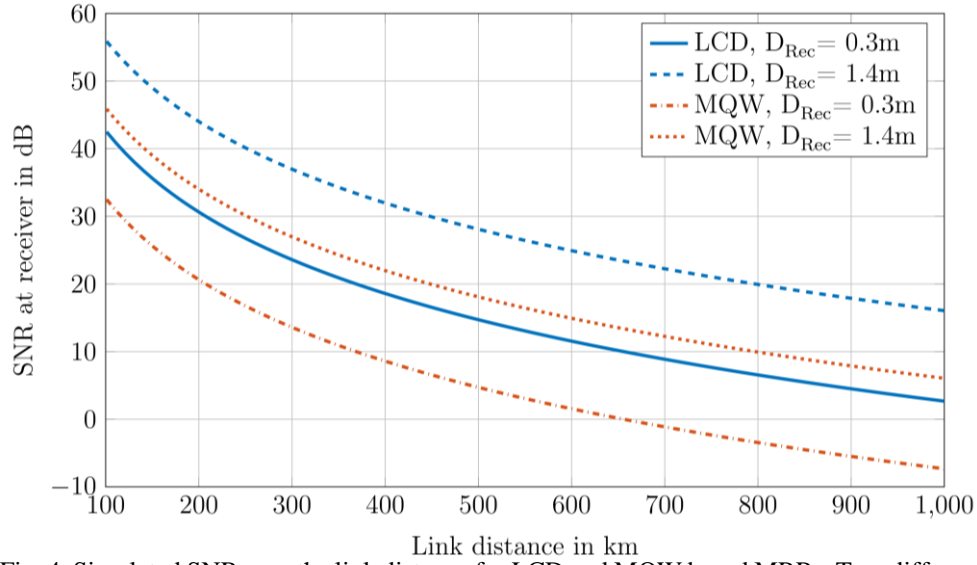
Fig. 4. Simulated SNR over the link distance for LCD and MQW based MRRs. Two different receiving telescope diameters are shown.

3. IMPLEMENTATION OF THE EXPERIMENTAL SETUP

Fig. 5 shows a schematic representation of the optical setup used to verify the feasibility of the proposed R-FSO-C setup. It includes a ground station which provides a laser source, beam steering mechanics and a receiving photo-detector. The MRR assembly is equipped with a data source for modulation input. The performance of the setup is evaluated in a laboratory environment (Section 3) as well as in an outdoor environment (Section 4).
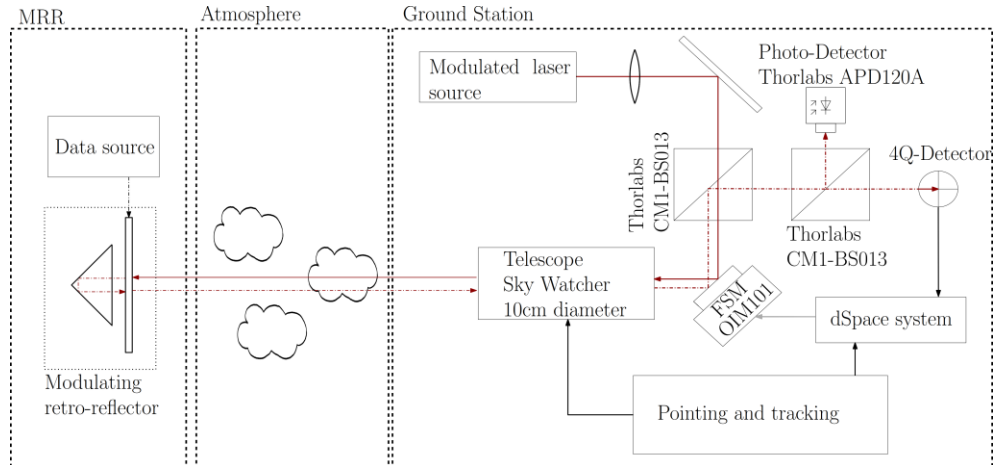

Fig. 5. Detailed schematic of the R-FSO-C test setup for evaluation of the proposed communication system.

The main component of the ground station is a SkyWatcher telescope (Sky-Watcher Black Diamond 100ED, Richmond) with an aperture size of 100 mm. It is used in a monostatic configuration (Fig. 6). A 1 mW laser diode with 635 nm is used. Two beam-splitters (Thorlabs CM1-BS013) split the received light onto two detectors. An avalanche photo- diode (Thorlabs APD120A2) is utilized as receiver for the transmitted data. A custom-made 4-quadrant photo-diode provides position feedback for the pointing and tracking system. For first test the system is used statically without actuation of the FSM or the telescope. A communication distance of up to 70 m is realized between buildings of Vienna University of Technology.

Fig. 6. Picture of the ground station and the plant.

The MRR is mounted stationary. All measurements are performed at night and with a visible wavelength (635 nm) to simplify alignment. The received data are recorded by means of a high-speed data acquisition system (Red Pitaya). Demodulation and data quality analysis are done in post processing with Matlab.

The MRR is an assembly of a corner-cube retro-reflector (Excel 1013A, Santa Clara) and a LCD (Toshiba FPB-AG03). The LCD is upcycled from 3D-shutter glasses. It provides a large, one-pixel area which can be driven by input voltages below 20 V. The LCD offers a high contrast ratio (> 1:100) and a wide field of view (> 30°). Furthermore, the power consumption of the LCD is low. A simple non-inverting operational amplifier circuit allows a power consumption of below 80 mW. Drawback of the LCD is its limited switching frequency of below 500 Hz. Assuming on/off-keying modulation the data-rate would be limited to 500 bps. Therefore, an optimized modulation principle is proposed. As the display is limited in its switching frequency the it is proposed to reduce the amount of necessary switching cycles per transmitted amount of data. In Fig. 7 the LCD's switching times are marked with t_{fast} and t_{slow}. Fig. 8 shows the histogram of the switching time of the LCD's fast edge. The jitter (standard deviation) of this switching time is shown to be as small as 0.17 us. This property allows utilization of digital pulse interval modulation (DPIM) [24]. DPIM defines transmitted information in the relative time difference between two consecutive pulses. In case of the LCD two consecutive fast edges are used to define this information. As the jitter of these edges is low, more information can be transmitted using less switching cycles. For the implementation the time is divided into slots and the number of time-slots between two fast edges of the LCD defines the data symbol.

For a time-slot width defined by 5σ, the data-rate calculates to approximately 3 kbps at an average switching frequency of 300 Hz. This estimation assumes equal distribution of all data symbols. With the LCD specific setup time t_{setup} (the minimum amount of time the LCD needs recover) and a time-slot width t_{slot}, specifying the time difference between two different symbols, the average cycle time of the DPIM modulated signal can be estimated with
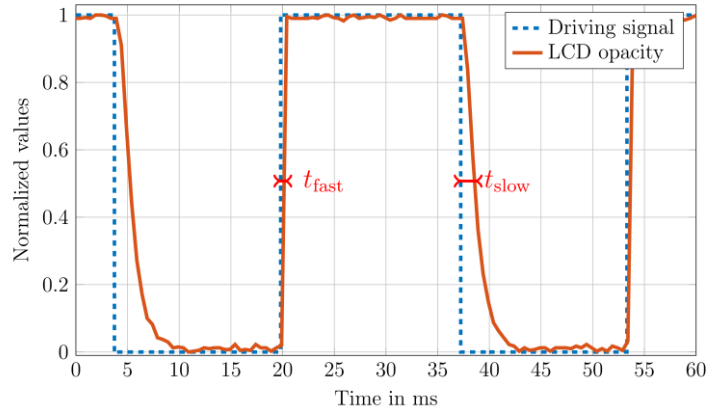

Fig. 7. Switching behavior of the LCD at 10 V rectangular input voltage. The switching times of the fast (t_{fast} = 0.28 ms) and the slow (t_{slow} = 1.8 ms) edge are marked.

$$\overline{t_{cycle}} = t_{setup} + t_{slot} \cdot \frac{S_{max}}{2}, \tag{11}$$

where S_{max} is the total number of transmittable symbols. The data-rate DR is calculated using the logarithm dualis of S_{max} and the cycle frequency

$$DR = \frac{1}{\overline{t_{cycle}}} \cdot log_2(S_{max}). \tag{12}$$

Assuming a setup time t_{setup} of 2.5 ms and a time-slot width of $t_{slot} = 0.17 \, us \cdot 5 \cdot 2 = 1.7 us$ (5σ), the data-rate is maximized to approximately 3 kbps at 550 transmittable symbols.

As the information is encoded in a pulse's position, every jitter source of the communication system may affect the overall performance. It is shown that no significant contribution to the overall jitter is given by the system's components, except the laser modulation at the GS. Internal reflections caused by the optical setup, as well as external

reflections caused by different atmospheric layers, require a modulated laser carrier-signal. This modulation uses short laser pulses (<200 ns) with a repetition rate of 100 kHz. This pulsed laser carrier-signal causes an increased uncertainty in terms of time position and therefore increases the overall jitter of the system. Therefore, the full system jitter is his higher with a value of 0.7 us. Compared to the average switching cycle time of approximately 3 ms the jitter of 0.7 us is still low. A maximum data-rate of 2.9 kbps is estimated assuming a time slot width defined by 5σ.
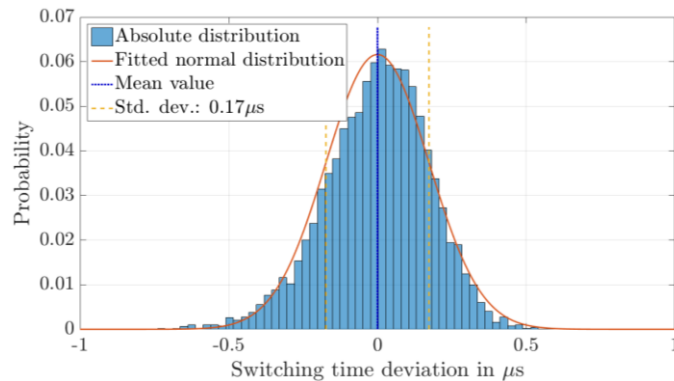

Fig. 8. Jitter (standard deviation) of the switching time t_{fast} of the LCD's fast edge. 25000 edges are captured and analyzed.

To verify the calculated values indoor measurements are performed. The setup shown in Fig. 5 is modified for this measurement. The telescope is removed and the MRR integrated into the setup at a distance of 30 cm. The pointing and tracking system is not active. No artificial disturbance is added to the signal path. A setup time of 1.93 ms and a time-slot width of 10 us are chosen. This configuration allows a maximum data-rate of 2.72 kbps at 106 transmittable symbols. No errors are found in the transmitted data-set of a long term measurement and a BER of below 10e-3 is confirmed with a confidence level of 0.9.

4. OUTDOOR EXPERIMENT RESULTS

To further verify the results of the system analysis and the estimations for data-rate, outdoor experiments are performed with the R-FSO-C setup presented in Section 3. The measurements are executed with the pulsed laser carrier signal described previously. The pointing and tracking system is not active. The outdoor measurements are performed between two buildings of Vienna University of Technology. Fig. 9 shows an overview of used site. The used configuration with low laser power is chosen to achieve similar SNR as estimated in Section 2. The simulated SNR (24 dB) of the LCD-MRR at a link distance of 300 km is taken as reference value. A data-rate of 2.53 kbps allows a higher time slot width, to optimize the link quality under turbulence induced disturbance. A long time measurement with this data-rate over a link distance of 70 m reveals no errors in the transmitted data (data not shown).

Fig. 9. Google maps view of the outdoor measurement location.

In summary the outdoor experiments successfully demonstrate the applicability of a LCD based MRR for R-FSO-C. The data-rate of 2.53 kbps achieved over a link distance of 70 m is in good agreement with the simulation.

5. CONCLUSION

This paper provides an analysis of the applicability of R-FSO-C for PNS. It shows the feasibility of R-FSO-C for PNS, utilizing off the shelf components. It is shown by simulation, that with an aperture size of 0.3 m of the transmitting and receiving telescope, a link distance of 300 km and a MRR aperture size of 2.54 cm, data-rates of 2.5 kbps using a LCD based MRR and 1 Mbps using a multi-quantum well modulator (MQW), seem achievable for PNS.

To verify the simulated performance a LCD-based MRR is evaluated as a possible modulator for R-FSO-C for PNS. An optimized modulation principle is proposed, which considers the very low switching time jitter (< 200 ns) of the LCD and therefore overcomes its limited switching frequency. Outdoor measurements between two roof decks at a data-rate of 2.5kbps and only 1 mW laser power confirm the proposed concept. It is shown, that a LCD-MRR can be

a competitive alternative to RF based communication modules for PNS. Especially the low power consumption of only 80 mW allows straightforward integration of this system into PNS. As part of future research, the LCD could easily be replaced with a more advanced modulator (e.g. MQW), which allows several orders of magnitude higher data rates using a similar setup.

6.   ACKNOWLEDGMENTS

7.   REFERENCES

[1]   J. Thoemel and F. Singarayar, *Status of the QB50 Cubesat Constellation Mission,* 65th International Astronautical Congress, Toronto, 2014.

[2]   J. Bouwmeester and J. Guo, *Survey of worldwide pico- and nanosatellite missions, distributions and subsystem technology,* Acta Astronautica, vol. 67, no. 7-8, pp. 854-862, 7-8 67 2010.

[3]   B. Buchen, *SpaceWorks 2014 Nano- Microsatellite Market Assessment,* AIAA/USU Conference on Small Satellites, 2014.

[4]   TU Graz IKS, *Brite Austria, TUG SAT-1,* TU Graz, http://www.tugsat.tugraz.at/tugsat-1. [Accessed 05 2016].

[5]   A. K. Majumdar, *Advanced Free Space Optics,* Springer, 2015.

[6]   B. Klofas and J. Anderson, *A Survey of CubeSat Communication Systems: 2009 - 2012,* in 10th Annual CubeSat Developers Workshop, San Luis Obispo, 2013.

[7]   B. Klofas and K. Leveque, *The Future of CubeSat Communications: Transitioning Away from Amateur Radio Frequencies for High-speed Downlinks,* AMSAT Space Symposium, vol. September, 2012.

[8]   A. Alonso, *Performance of satellite-to-ground-communications link between ARTEMIS and the Optical Ground Station,* Proc. SPIE, Optics in Atmospheric Propagation and Adaptive Systems, vol. VII, no. 5572, 2004.

[9]   M. Thoyoshima, T. Kuri and W. Klaus, *Overview of the laser communication system for the NICT optical ground station and laser communication experiments on ground-to-satellite links,* Journal of the National Institute of Information and Communications Technology, vol. 59, no. 1-2, pp. 53-75, 2012.

[10] T. Tolker-Nielsen and J.-C. Guillen, *Silex: The First European Optical Communication Terminal in Orbit,* in ESA Bulletin 96, 1998.

[11] G. Jensen and C. Swenson, *A Laser Downlink for Small Satellites Using an Optically Modulating Retroreflector,* Small Satellite Conference, 1992.

[12] F. J. López-Hernández, M. A. Geday, and G. Del-Campo, *Ground-to-Survey Aerostatic Platform Bidirectional Free-Space Optical Link,* Proceedings of SPIE, vol. 6736, no. September, 2007.

[13] W. S. Rabinovich, P. G. Gotz, R. Mahon and et al., *45-Mbit/s cat's-eye modulating retroreflectors,* Optical Engineering, vol. 46, no. October, 2007.

[14] M. L. Plett, *Free-Space Optical Communication Link Across 16 Kilometers to a Modulated Retro-Reflector Array,* Ph.D. Dissertation, University of Maryland, 2007.

[15] J. Stupl and J. Mason, *Modulating Retro-Reflectors: Technology, Link Budgets and Applications,* in 63rd International Astronautical Congress, Naples, 2012.

[16] P. G. Goetz, W. S. Rabinovich, G. C. Gilbreath et al., *Multiple quantum well based modulating retroreflectors for inter- and intra-spacecraft communication,* Proceedings of SPIE, vol. 6308, no. 06, 2006.

[17] H. Henninger and O. Wilfert, *An introduction to free-space optical communications,* Radio Engineering, vol. 19, no. 2, pp. 203-212, 2010.

[18] G. D. Roth, *Handook of Practial Astronomy,* Springer, 2009.

[19] W. Romanishin, *An Introduction to Astronomical Photometry Using CCDs,* University of Oklahoma: Romanishin, W., 2002.

[20] T. Y. Elganimi, *Performance Comparison between OOK, PPM and PAM Modulation Schemes for Free Space Optical (FSO) Communication Systems: Analytical Study,* International Journal of Computer Applications, vol. 79, no. 11, pp. 22-27, 2013.

[21] P. Muri and J. McNair, *A Survey of Communication Sub-systems for Intersatellite Linked Systems and Cubesat Missions,* Journal of Communications, vol. 7, no. 4, pp. 290-308, 2012.

[22] W. Rabinovich, P. M. R. Goetz et al., *Performance of Cat's eye modulating retro-reflectors for free-space optical communications,* Naval Research Laboratory, Washington DC, 2004.

[23] K. Sayyah, A. Narayanan, D. Persechini et al., *Conformal Pixellated MQW Modulator Structure for Modulating Retroreflector Applications,* IEEE Photonics Technology Letters, vol. 17, no. 9, pp. 1854-1856, 2005.

[24] E. Kaluarachi, Z. Ghassemlooy and B. Wilson, *Digital pulse interval modulation for optical free space communication links,* in IEEE Colloq. On Optical Free Space Communication Links, London, 1996.

[25] H. Heidt and J. Puig-Suari, *A new Generation of Picosatellite for Education and Industry Low-Cost Space Experimentation,* AIAA/USU Conference on Small Satellites, 2000.

[26] H. Hemmati, *Interplanetary Laser Communications,* Optics and Photonics, vol. 18, no. November, pp. 22-27, 2007.

[27] QB50, *QB50 Mission Objectives,* QB50, 2016.

[28] P. Muri and J. McNair, *A Survey of Communication Sub-systems for Intersatellite Linked Systems and Cubesat Missions,* Journal of Communications, vol. 4, no. 7, pp. 290-308, 4 7 2012.

[29] W. Feller, *An Introduction to Probability Theory and its Applications,* New York: John Wiley and Sons, 1965.